



HAL
open science

Decentralized optimal control of a vehicle platoon with guaranteed string stability

Fabio Morbidi, Patrizio Colaneri, Thomas Stanger

► **To cite this version:**

Fabio Morbidi, Patrizio Colaneri, Thomas Stanger. Decentralized optimal control of a vehicle platoon with guaranteed string stability. ECC 2013 - 12th biannual European Control Conference, Jul 2013, Zurich, Switzerland. pp.3494-3499. hal-00961553

HAL Id: hal-00961553

<https://hal.science/hal-00961553>

Submitted on 24 Mar 2014

HAL is a multi-disciplinary open access archive for the deposit and dissemination of scientific research documents, whether they are published or not. The documents may come from teaching and research institutions in France or abroad, or from public or private research centers.

L'archive ouverte pluridisciplinaire **HAL**, est destinée au dépôt et à la diffusion de documents scientifiques de niveau recherche, publiés ou non, émanant des établissements d'enseignement et de recherche français ou étrangers, des laboratoires publics ou privés.

Decentralized optimal control of a car platoon with guaranteed string stability

Fabio Morbidi, Patrizio Colaneri, Thomas Stanger

Abstract— This paper presents new *decentralized optimal strategies for Cooperative Adaptive Cruise Control (CACC) of a car platoon under string-stability constraints*. Two related scenarios are explored in the article: in the first one, a linear-quadratic regulator in the presence of measurable disturbances is synthesized, and the string-stability of the platoon is enforced over the controller’s feedback and feedforward gains. In the second scenario, H_2 - and H_∞ -performance criteria, respectively accounting for the desired group behavior and the string-stability of the platoon, are simultaneously achieved using the recently-proposed *compensator blending method*. An analytical study of the impact of actuation/communication delays and uncertain model parameters on the stability of the multi-vehicle system, is also conducted. The theory is illustrated via numerical simulations.

I. INTRODUCTION

A. Motivation and related work

Traffic congestion has become a serious issue in modern cities’ life. In 2010, congestion caused urban Americans to travel 4.8 billion hours more and to purchase an extra 1.9 billion gallons of fuel, for a congestion cost of \$101 billion [1]. Because of such a big impact on productivity, pollution and human welfare, a considerable effort has been devoted in the last decades toward devising innovative systems which may reduce traffic jams and improve driver’s safety and comfort. This research activity, together with numerous “intelligent highway” initiatives in the U.S. (e.g., California PATH research program), Japan and Europe, has led to the development of *Adaptive Cruise Control (ACC)* systems, currently available in numerous sedans, and lately to the design of *Cooperative Adaptive Cruise Control (CACC)* systems which extend the functionality of ACC by leveraging the information exchanged via vehicle-to-vehicle and/or vehicle-to-infrastructure wireless communication.

The idea of using *optimization-based* policies for CACC is not new and dates back at least to the end of 90s. In [2] the longitudinal control of each car is computed using a gradient-based descent algorithm, and no communication with the leading vehicle of the platoon is needed. In [3] a decentralized overlapping controller is developed using the inclusion principle: possible extensions to the basic scenario are also discussed, comprising the use of reduced-order observers for estimating the state of the preceding vehicle and the identification of suitable stability-preserving conditions. A similar control framework is adopted in [4], where the authors analyze the impact of range-limited sensing, assuming that the lead car broadcasts its state information, i.e. its speed and acceleration information, to all platoon members. Recently, we have witnessed a growing interest in

CACC based on *Model Predictive Control (MPC)*. In [5] an explicit MPC controller for “Stop-&-Go” ACC is synthesized, and its performance is evaluated by distinguishing between comfort of the resulting longitudinal vehicle behavior and behavior due to the traffic constraints. A similar MPC approach is considered in [6], where the tuning of the cruise controller is made simple by the parameterization of multiple performance indices. In [7], a multi-objective MPC-based CACC strategy is developed for multiple trucks and tested in realistic traffic conditions. An analogous setup is considered in [8], where the performance of MPC is compared with that of a PD and a sliding-mode controller, in a real driving cycle.

A significant stream of research in the CACC literature has also focused on robustness and stability issues, and notably on the so-called *string stability* of a car platoon. A platoon is said string stable under an assigned control policy, if oscillations are attenuated upstream the traffic flow. In [9], [10], early studies were conducted concerning the effect of communication delays on the string stability. A similar analysis has been recently carried out in [11] in the frequency domain with heterogeneous vehicles, under a simple PD control. In [12], sufficient conditions are given that imply a lower bound on the peak of the frequency-response magnitude of the transfer function mapping a disturbance to the leading vehicle to a vehicle in the chain. This bound quantifies the effect of spacing policy, inter-vehicle communication policy, and vehicle settling response performance. Finally, in [13], the problem of regulating inter-vehicle distances in a car platoon is approached from a networked-system perspective. Tradeoffs between CACC performance and network specifications are pointed out, and a study of the impact of network-induced effects on string stability is conducted.

B. Original contributions and organization

After an introductory section devoted to the modeling of the car platoon that we adapted from [7], Sect. III presents original results concerning the *decentralized optimal CACC* of a team of n vehicles under string-stability constraints and a constant-time headway spacing policy. The CACC problem is approached here from two different perspectives. In the first scenario, an infinite-time linear-quadratic regulator in the presence of measurable disturbances is synthesized and the string-stability of the platoon is enforced over the regulator’s feedback and feedforward gains. In the second scenario, we simultaneously achieve H_2 - and H_∞ -performance criteria, which respectively dictate the desired group behavior and string-stable behavior of the platoon, by using the *compensator blending method* recently proposed in [14]. This method is more intuitive and simpler to implement than the classical recursive approaches to mixed H_2/H_∞ optimal control [15], lately used in [16] to design a constant-spacing CACC strategy for a chain of trucks.

It is worth pointing out here that unlike the MPC methods described in Sect. I-A, state and input constraints cannot be handled by the strategies described in this paper. However, differently from those methods, the relative simplicity of our

Fabio Morbidi and Thomas Stanger are with the Institute for Design and Control of Mechatronical Systems, Johannes Kepler University, Altenbergerstraße 69, 4040 Linz, Austria. Email: {fabio.morbidi, thomas.stanger}@jku.at

Present address of Fabio Morbidi: Networked Controlled System (NeCS) team, Inria Grenoble Rhône-Alpes, 655 Avenue de l’Europe, Montbonnot, 38334 Saint Ismier, France.

Patrizio Colaneri is with the Dipartimento di Elettronica e Informazione, Politecnico di Milano, Piazza Leonardo da Vinci 32, 20133 Milano, Italy. Email: colaneri@elet.polimi.it

The authors gratefully acknowledge the sponsoring of this work by the COMET K2 center “Austrian Center of Competence in Mechatronics”.

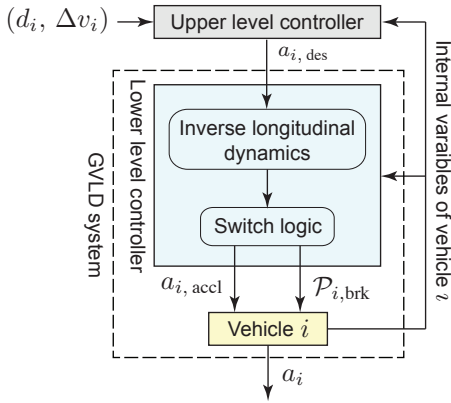


Fig. 1. Hierarchical control architecture of vehicle i . In the lower-level controller, a switching logic is adopted to avoid simultaneous actions from the drive train and braking system (see [7] for more details).

control design procedures allowed us to establish insightful *analytical conditions* for the solvability of the *optimal CACC* problem with string stability, both in the “nominal case” and in the presence of actuation/communication delays and, for the first time, uncertain model parameters.

In Sect. IV, the proposed theoretical results are illustrated via numerical simulations, and finally, in Sect. V, the main contributions of the paper are summarized and possible avenues for future research are outlined.

II. MODELING OF THE PLATOON

A. Compensation of nonlinear longitudinal dynamics

In this paper we consider a platoon of n identical cars moving in one dimension, where vehicle 1 is the *leader* of the platoon and $v_1, a_1, \dots, v_n, a_n$ denote the velocity and acceleration of the n cars, respectively. In the following, we will assume that a_1 is an *assigned* acceleration profile.

As it is known, the longitudinal dynamics of a car is nonlinear and its main features include the static nonlinearity of engine torque maps, time-varying gear position and aerodynamic drag force. Following [7], we will avail ourselves of a *lower-level* and an *upper-level* controller, as illustrated in Fig. 1. The lower-level controller determines the value of the accelerator pedal position ($a_{i,\text{accl}}$) and brake pressure ($\mathcal{P}_{i,\text{brk}}$) of i -th car, $i \in \{2, \dots, n\}$, so that the desired acceleration $a_{i,\text{des}}$ is tracked by the actual acceleration a_i . On the other end, the upper level controller determines the desired longitudinal acceleration according to the inter-vehicle and vehicle i 's internal variables, which include the engine speed, gear ratio and car's speed and acceleration. We assume that the internal variables are all measured by the on-board car sensors (cf. Fig. 1).

The inter-vehicle variables are the relative distance d_i between vehicle $i-1$ and vehicle i and the speed error $\Delta v_i = v_{i-1} - v_i$, which are measured by a radar mounted in front of the car. When designing the lower-level controller, one of the challenges is the presence of several nonlinearities coming from engine, transmission, and aerodynamic drag. To compensate for them, following [7], the inverse-dynamics control design method is used here. The lower-level controller together with vehicle i , then yield a new plant with input $a_{i,\text{des}}$ and output a_i , called *Generalized Vehicle Longitudinal Dynamic (GVLD)* system, described by,

$$a_i(s) = \frac{K_L}{T_L s + 1} a_{i,\text{des}}(s), \quad i \in \{2, \dots, n\}, \quad (1)$$

where $K_L > 0$ is the system gain (ideally equal to 1), and T_L is the time constant of GVLD.

B. Car-following model

In order to design the *upper-level controller*, a car-following model is built by combining the GVLD system and the inter-vehicular longitudinal dynamics. For the inter-vehicular dynamics, two state variables are of interest: the *clearance error* $\Delta d_i(t) = d_i(t) - d_{i,\text{des}}(t)$ and the speed error Δv_i , where $d_{i,\text{des}}(t)$ denotes driver's *desired inter-vehicle distance* (cf. [7]). Various models for $d_{i,\text{des}}$ have been proposed in the literature: in this paper, we adopt the popular *constant-time headway* spacing policy $d_{i,\text{des}}(t) = \tau_h v_i(t) + d_0$, where τ_h is the *nominal time headway* and d_0 is the *desired distance at standstill* [11].

Note that d_0 can be regarded as an extension of the length ℓ_i of vehicle i (cf. [11] and see Fig. 2), and we can redefine the vehicle's length as $\ell'_i = \ell_i + d_0$. Hence, d_0 will be neglected in the rest of the paper. By collecting the inter-vehicular dynamics and equation (1) together, we end up with the following linear time-invariant system [7],

$$\dot{\mathbf{x}}_i = \mathbf{A} \mathbf{x}_i + \mathbf{B} u_i + \mathbf{G} z_i, \quad i \in \{2, \dots, n\}, \quad (2)$$

where

$$\mathbf{A} = \begin{bmatrix} 0 & 1 & -\tau_h \\ 0 & 0 & -1 \\ 0 & 0 & -1/T_L \end{bmatrix}, \quad \mathbf{B} = \begin{bmatrix} 0 \\ 0 \\ K_L/T_L \end{bmatrix}, \quad \mathbf{G} = \begin{bmatrix} 0 \\ 1 \\ 0 \end{bmatrix}, \quad (3)$$

$\mathbf{x}_i = [\Delta d_i, \Delta v_i, a_i]^T \in \mathbb{R}^3$ is the state of the system, $u_i = a_{i,\text{des}} \in \mathbb{R}$ is the control input, and $z_i = a_{i-1} \in \mathbb{R}$ is a measurable disturbance. In the following, we will assume the transmission of the acceleration a_{i-1} from vehicle $i-1$ to vehicle i .

III. STRING-STABLE OPTIMAL CACC

In this section, we present two *decentralized* optimal CACC strategies (see Sect. III-A and Sect. III-B, respectively), which preserve the string stability of the car platoon.

A. LQ regulation with guaranteed string stability

In order to specify the desired behavior of the platoon, let us introduce the following optimal control problem,

$$\begin{aligned} \min_{u_i} \quad & \int_0^\infty (\mathbf{x}_i^T \mathbf{Q} \mathbf{x}_i + r u_i^2) dt, \quad i \in \{2, \dots, n\}, \\ \text{s.t.} \quad & \dot{\mathbf{x}}_i = \mathbf{A} \mathbf{x}_i + \mathbf{B} u_i + \mathbf{G} z_i, \end{aligned} \quad (4)$$

where $\mathbf{Q} \succeq \mathbf{0}$ and $r > 0$ are suitable weights on the state \mathbf{x}_i and input u_i of system (2). This is an infinite-time linear-quadratic (LQ) regulation problem in the presence of the measurable disturbance z_i . If we assume that z_i is constant (cf. [3]), this problem admits the following closed-form solution [17, Sect. 4.3],

$$u_i^* = -r^{-1} \mathbf{B}^T (\mathbf{P} \mathbf{x}_i + \mathbf{q}_i), \quad (5)$$

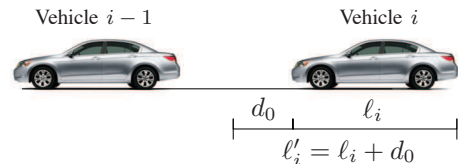


Fig. 2. Two vehicles in the platoon: ℓ_i is the actual length of vehicle i , d_0 is the desired distance at standstill, and $\ell'_i = \ell_i + d_0$ is the “extended length” of vehicle i that we will use in our analysis in Sect. III.

where $\mathbf{P} \succeq \mathbf{0}$ is the solution of the algebraic Riccati equation,

$$\mathbf{P} \mathbf{A} + \mathbf{A}^T \mathbf{P} - r^{-1} \mathbf{P} \mathbf{B} \mathbf{B}^T \mathbf{P} + \mathbf{Q} = \mathbf{0},$$

and $\mathbf{q}_i = [(\mathbf{A} - r^{-1} \mathbf{B} \mathbf{B}^T \mathbf{P})^T]^{-1} \mathbf{P} \mathbf{G} z_i$. Note that the control law (5) can be rewritten more compactly as,

$$u_i^* = \mathbf{k}^T \mathbf{x}_i + k_F z_i, \quad (6)$$

where

$$\begin{aligned} \mathbf{k}^T &= [k_1, k_2, k_3] \triangleq -r^{-1} \mathbf{B}^T \mathbf{P}, \\ k_F &\triangleq -r^{-1} \mathbf{B}^T [(\mathbf{A} - r^{-1} \mathbf{B} \mathbf{B}^T \mathbf{P})^T]^{-1} \mathbf{P} \mathbf{G}. \end{aligned} \quad (7)$$

By substituting equation (6) into system (2), we finally obtain the following closed-loop dynamics,

$$\dot{\mathbf{x}}_i = (\mathbf{A} + \mathbf{B} \mathbf{k}^T) \mathbf{x}_i + (\mathbf{B} k_F + \mathbf{G}) z_i, \quad (8)$$

which is the basis for our forthcoming developments.

The following definition introduces the notion of string stability used through the paper.

Definition 1 (*String stability* [11]): Consider the following transfer function,

$$\Lambda_i(s) = \frac{a_i(s)}{a_{i-1}(s)}, \quad i \in \{2, \dots, n\}, \quad (9)$$

where $a_i(s)$ and $a_{i-1}(s)$, as in Sect. II-A, denote the Laplace transforms of the acceleration signals $a_i(t)$ and $a_{i-1}(t)$, respectively. A sufficient condition for the *string stability* of a platoon of n identical cars is that,

$$\|\Lambda_i(j\omega)\|_\infty \leq 1, \quad i \in \{2, \dots, n\}, \quad (10)$$

where $\|\Lambda_i(j\omega)\|_\infty \triangleq \sup_\omega |\Lambda_i(j\omega)|$ denotes the H_∞ norm of the transfer function in (9). \diamond

In other words, the longitudinal dynamics of a platoon is string stable whether oscillations are not amplified upstream the traffic flow. The next proposition provides sufficient conditions on the feedback and feedforward control gains in (7), for the string stability of the car platoon. These conditions are successively extended to the case of constant *communication delays* among the vehicles and within the individual GVLD systems.

Proposition 1 (*String-stability conditions*): Consider system (8). The car platoon is string stable if the following two inequalities are satisfied:

$$\begin{aligned} (K_L k_3 - 1)^2 - 2 T_L K_L (\tau_h k_1 + k_2) - K_L^2 k_F^2 &\geq 0, \\ 2k_1 (K_L k_3 - 1) + k_1 K_L (\tau_h^2 k_1 + 2(\tau_h k_2 + k_F)) &\geq 0. \end{aligned} \quad (11)$$

Proof: The last of the three (scalar) differential equations in (8), is:

$$\dot{a}_i = \left(\frac{K_L k_3 - 1}{T_L} \right) a_i + \frac{K_L}{T_L} [k_1 \Delta d_i + k_2 \Delta v_i + k_F a_{i-1}].$$

In the Laplace domain (assuming $a_i(0) = 0$), this equation becomes:

$$\begin{aligned} \left[s - \left(\frac{K_L k_3 - 1}{T_L} \right) \right] a_i(s) &= \frac{K_L}{T_L} [k_1 \Delta d_i(s) \\ &+ k_2 \Delta v_i(s) + k_F a_{i-1}(s)]. \end{aligned} \quad (12)$$

Note now that

$$\Delta d_i(s) = \frac{a_{i-1}(s) - a_i(s)}{s^2} - \frac{\tau_h a_i(s)}{s}, \quad \Delta v_i(s) = \frac{a_{i-1}(s) - a_i(s)}{s}. \quad (13)$$

By plugging (13) into (12) and collecting similar terms together, after simple algebraic manipulations, we get:

$$\Lambda_i(s) = \frac{K_L (k_1 + k_2 s + k_F s^2)}{T_L s^3 - (K_L k_3 - 1) s^2 + (\tau_h k_1 + k_2) K_L s + K_L k_1}. \quad (14)$$

If we now impose the condition $|\Lambda_i(j\omega)| \leq 1, \forall \omega > 0$, we end up with the following inequality in the variable ω :

$$\begin{aligned} T_L^2 \omega^4 + [(K_L k_3 - 1)^2 - 2 T_L K_L (\tau_h k_1 + k_2) - K_L^2 k_F^2] \omega^2 + \\ 2 K_L k_1 (K_L k_3 - 1) + [(\tau_h k_1 + k_2)^2 + 2 k_1 k_F - k_2^2] K_L^2 &\geq 0. \end{aligned} \quad (15)$$

A sufficient condition for the nonnegativity of the fourth-order polynomial on the left-hand side of (15), is that all its coefficients are nonnegative. This leads to (11). \blacksquare

Note that it is generally possible to enforce the conditions in (11) by properly tuning the weights \mathbf{Q} and r in (4).

Next, we will try to repeat the previous analysis in the more challenging scenario in which the signal $z_i = a_{i-1}$ is transmitted between vehicle $i - 1$ and vehicle i with a constant delay θ , and that a constant actuator's communication delay ϕ is present in the GVLD system. It is immediate to verify that under these conditions, equation (2), for $i \in \{2, \dots, n\}$, transforms into:

$$\dot{\mathbf{x}}_i(t) = \mathbf{A} \mathbf{x}_i(t) + \mathbf{B} u_i(t - \phi) + \mathbf{G} z_i(t - \theta). \quad (16)$$

Let us now choose a control input of the form,

$$u_i(t) = \mathbf{k}^T \mathbf{x}_i(t) + k_F z_i(t - \theta). \quad (17)$$

Following the same outline of the proof of Prop. 1, from (16) we obtain $[s - (\frac{K_L k_3 e^{-\phi s} - 1}{T_L})] a_i(s) = \frac{K_L}{T_L} e^{-\phi s} [k_1 \Delta d_i(s) + k_2 \Delta v_i(s) + k_F a_{i-1}(s) e^{-\theta s}]$. By using (13), we get the transfer function:

$$\Lambda_i(s) = \frac{K_L e^{-\phi s} (k_1 + k_2 s + k_F s^2 e^{-\theta s})}{T_L s^3 + s^2 + K_L e^{-\phi s} [-k_3 s^2 + (k_1 \tau_h + k_2) s + k_1]}$$

If we now impose $|\Lambda_i(j\omega)| \leq 1, \forall \omega > 0$, we obtain the following quasipolynomial inequality in the variable ω :

$$\begin{aligned} T_L^2 \omega^4 + 2 K_L k_3 T_L \sin(\phi \omega) \omega^3 + [1 + (k_3^2 - k_F^2) K_L^2 \\ - 2 K_L \cos(\phi \omega) (k_3 + T_L (k_1 \tau_h + k_2))] \omega^2 \\ - 2 [k_2 k_F K_L^2 \sin(\theta \omega) + K_L \sin(\phi \omega) (k_1 (\tau_h - T_L) + k_2)] \omega \\ + K_L [-k_2^2 K_L + 2 k_1 K_L k_F \cos(\theta \omega) + 2 K_L k_1 k_3 \\ + K_L (k_1 \tau_h + k_2)^2 - 2 k_1 \cos(\phi \omega)] &\geq 0. \end{aligned} \quad (18)$$

The study of the feasibility of (18) is made complicated by the presence of the sinusoidal and cosinusoidal terms, and suitable approximations to these functions need to be introduced in order to establish conditions on the gains of controller (17), similar to those in (11). A simple option, consists of using the following Maclaurin series expansions of the cosine and sine functions $\cos(\alpha\omega) \simeq 1 - (\alpha\omega)^2/2!$, $\sin(\alpha\omega) \simeq \alpha\omega - (\alpha\omega)^3/3!$, $\alpha \in \{\theta, \phi\}$, under the assumption of "small" $\alpha\omega$. Inequality (18) can thus be rewritten as:

$$\begin{aligned} -\frac{1}{3} K_L k_3 T_L \phi^3 \omega^6 + \{T_L^2 + 2 K_L k_3 T_L \phi + K_L [k_3 + T_L (k_1 \tau_h \\ + k_2)] \theta^2 + \frac{1}{3} [k_2 k_F K_L^2 \theta^3 + K_L (k_1 (\tau_h - T_L) + k_2) \phi^3]\} \omega^4 \\ + \{(K_L k_3 - 1)^2 - 2 T_L K_L (\tau_h k_1 + k_2) - K_L^2 k_F^2 \\ - K_L^2 k_F \theta (2k_2 + \theta k_1) - 2 K_L [k_2 + k_1 (\tau_h - T_L)] \phi \\ + K_L k_1 \phi^2\} \omega^2 + 2 K_L k_1 (K_L k_3 - 1) \\ + k_1 K_L^2 [\tau_h^2 k_1 + 2(\tau_h k_2 + k_F)] &\geq 0. \end{aligned} \quad (19)$$

A sufficient condition for the nonnegativity of the six-order polynomial on the left-hand side of (19), is that all its coefficients are nonnegative, from which we deduce the following four inequalities:

$$\begin{aligned}
& -k_3 \phi^3 \geq 0, \\
& T_L^2 + 2K_L k_3 T_L \phi + K_L [k_3 + T_L (k_1 \tau_h + k_2)] \theta^2 \\
& + \frac{1}{3} [k_2 k_F K_L^2 \theta^3 + K_L (k_1 \tau_h + k_2 - k_1 T_L) \phi^3] \geq 0, \\
& (K_L k_3 - 1)^2 - 2 T_L K_L (\tau_h k_1 + k_2) - K_L^2 k_F^2 - K_L^2 k_F \theta \cdot \\
& (2k_2 + \theta k_1) - 2K_L [k_2 + k_1 (\tau_h - T_L)] \phi + K_L k_1 \phi^2 \geq 0, \\
& 2k_1 (K_L k_3 - 1) + k_1 K_L (\tau_h^2 k_1 + 2(\tau_h k_2 + k_F)) \geq 0.
\end{aligned}$$

These inequalities are approximate sufficient conditions for the string stability of the car platoon in the presence of the constant communication delays θ and ϕ .

B. Simultaneous H_2 - and H_∞ -performance achievement via compensator blending

In this section, we present a decentralized CACC strategy alternative to that considered in Sect. III-A. By relying on the *compensator blending* method proposed in [14], we are here interested in jointly solving two problems: minimize the H_2 -performance index in (4) and achieve an H_∞ criterium (cf. equation (10)) accounting for the string-stable behavior of the platoon. We will separately design the H_2 and H_∞ control laws $u_i = \mathbf{k}_2^T \mathbf{x}_i$, $u_i = \mathbf{k}_\infty^T \mathbf{x}_i$, $i \in \{2, \dots, n\}$, and obtain a (dynamic) compensator of the form,

$$\mathcal{K}_i : \begin{cases} \dot{\mathbf{z}}_i = \mathbf{A}_{\mathcal{K},i} \mathbf{z}_i + \mathbf{B}_{\mathcal{K},i} \mathbf{x}_i, \\ u_i = \mathbf{C}_{\mathcal{K},i} \mathbf{z}_i + \mathbf{D}_{\mathcal{K},i} \mathbf{x}_i, \end{cases} \quad (20)$$

which *simultaneously* fulfills the H_2 and H_∞ criteria. To this end, let us introduce the following system,

$$\mathcal{G}_i : \begin{cases} \dot{\mathbf{x}}_i = \mathbf{A} \mathbf{x}_i + \mathbf{B} u_i + \mathbf{x}_i(0) z_{i,2} + \mathbf{G} z_{i,\infty}, \\ \mathbf{y}_{i,2} = \mathbf{C}_2 \mathbf{x}_i + \mathbf{D}_2 u_i, \quad i \in \{2, \dots, n\}, \\ \mathbf{y}_{i,\infty} = \mathbf{C}_\infty \mathbf{x}_i, \end{cases}$$

where

$$\begin{aligned}
z_{i,2}(t) &= \delta(t), \quad \mathbf{C}_2 = \begin{bmatrix} \mathbf{Q}^{1/2} \\ \mathbf{0}_{1 \times 3} \end{bmatrix}, \quad \mathbf{D}_2 = \begin{bmatrix} \mathbf{0}_{3 \times 1} \\ r^{1/2} \end{bmatrix}, \\
z_{i,\infty}(t) &= z_i(t), \quad \mathbf{C}_\infty = [0 \quad 0 \quad 1],
\end{aligned}$$

$\mathbf{x}_i(0)$ is the initial state, $\delta(t)$ is the Dirac's delta, $\mathbf{0}_{1 \times 3}$ is an 1×3 vector of zeros, and the subscripts "2" and " ∞ " refer to the H_2 - and H_∞ -performance indices, respectively. Note that the compensator blending procedure in [14], is valid under the assumption of a stabilizable pair (\mathbf{A}, \mathbf{B}) (in our specific case, (\mathbf{A}, \mathbf{B}) is indeed controllable, cf. (3)), and of full column-rank matrices $[\mathbf{x}_i(0) \quad \mathbf{G}]$, $i \in \{2, \dots, n\}$. An additional requirement is that \mathbf{k}_2 and \mathbf{k}_∞ are *stabilizing*.

Since the regulator \mathbf{k}_2 can be easily synthesized, in what follows we will limit ourselves to the design of the more challenging $\mathbf{k}_\infty = [k_{\infty,1}, k_{\infty,2}, k_{\infty,3}]^T$ (which we *cannot* straightforwardly calculate using state-of-the-art methods owing to our peculiar choice of the output matrix \mathbf{C}_∞). Note that the characteristic polynomial of matrix,

$$\hat{\mathbf{A}} = \mathbf{A} + \mathbf{B} \mathbf{k}_\infty^T = \begin{bmatrix} 0 & 1 & -\tau_h \\ 0 & 0 & -1 \\ \frac{K_L k_{\infty,1}}{T_L} & \frac{K_L k_{\infty,2}}{T_L} & \frac{K_L k_{\infty,3} - 1}{T_L} \end{bmatrix}, \quad (21)$$

is

$$\det(\lambda \mathbf{I}_3 - \hat{\mathbf{A}}) = \lambda^3 - \left(\frac{K_L k_{\infty,3} - 1}{T_L} \right) \lambda^2 + \frac{K_L}{T_L} (k_{\infty,1} \tau_h + k_{\infty,2}) \lambda + \frac{K_L}{T_L} k_{\infty,1}, \quad (22)$$

where \mathbf{I}_3 denotes the 3×3 identity matrix. Hence, from the Routh-Hurwitz stability criterion, $\hat{\mathbf{A}}$ is Hurwitz (and thus \mathbf{k}_∞

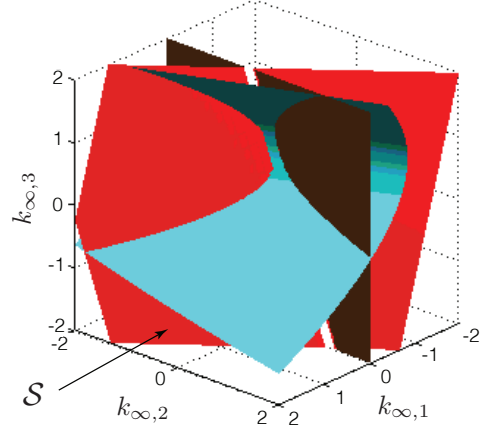


Fig. 3. The set \mathcal{S} of all feasible regulators \mathbf{k}_∞ in $[-2, 2]^3$, for $\tau_h = 2.5$, $K_L = 1$ and $T_L = 0.45$. For this parameters' selection, \mathcal{S} (in the front lower corner of the figure) is completely defined by the two inequalities in (24), depicted in cyan and red, respectively.

is stabilizing), if the following four inequalities are satisfied:

$$\begin{aligned}
& K_L k_{\infty,3} < 1, \quad k_{\infty,1} \tau_h + k_{\infty,2} > 0, \quad k_{\infty,1} > 0, \\
& (K_L k_{\infty,3} - 1)(k_{\infty,1} \tau_h + k_{\infty,2}) + k_{\infty,1} T_L < 0. \end{aligned} \quad (23)$$

Moreover, we have that (cf. equation (14)):

$$\begin{aligned}
\Lambda_i(s) &= \mathbf{C}_\infty (s \mathbf{I}_3 - \hat{\mathbf{A}})^{-1} \mathbf{G} = \\
& \frac{K_L (k_{\infty,1} + k_{\infty,2} s)}{T_L s^3 - (K_L k_{\infty,3} - 1) s^2 + (\tau_h k_{\infty,1} + k_{\infty,2}) K_L s + K_L k_{\infty,1}}.
\end{aligned}$$

If, as in the proof of Prop. 1, we now impose that $|\Lambda_i(j\omega)| \leq 1$, $\forall \omega > 0$, for string stability, we end up with the following two inequalities (which coincide with those in (11) for $k_F = 0$), which add to those in (23):

$$\begin{aligned}
& (K_L k_{\infty,3} - 1)^2 - 2 T_L K_L (\tau_h k_{\infty,1} + k_{\infty,2}) \geq 0, \\
& 2 k_{\infty,1} (K_L k_{\infty,3} - 1) + k_{\infty,1} K_L \tau_h (\tau_h k_{\infty,1} + 2 k_{\infty,2}) \geq 0. \end{aligned} \quad (24)$$

Note that (23)-(24) define the set $\mathcal{S} \subset \mathbb{R}^3$ of all feasible regulators \mathbf{k}_∞ : as illustrated in the example of Fig. 3, \mathcal{S} is a nonconvex set. Since \mathcal{S} contains infinite gain vectors, one needs an optimal criterion to select \mathbf{k}_∞ , such as, e.g., minimizing any vector norm. In the numerical simulations in Sect. IV-B, we chose the \mathbf{k}_∞ with minimum squared 2-norm.

Given the regulator \mathbf{k}_2 and a regulator $\mathbf{k}_\infty \in \mathcal{S}$, by using Procedure 2.1 in [14], the matrices $\mathbf{A}_{\mathcal{K},i}$, $\mathbf{B}_{\mathcal{K},i}$, $\mathbf{C}_{\mathcal{K},i}$, $\mathbf{D}_{\mathcal{K},i}$ of the compensator in (20) can be simply computed as,

$$\begin{bmatrix} \mathbf{D}_{\mathcal{K},i} & \mathbf{C}_{\mathcal{K},i} \\ \mathbf{B}_{\mathcal{K},i} & \mathbf{A}_{\mathcal{K},i} \end{bmatrix} = \begin{bmatrix} \mathbf{k}_2^T & \mathbf{k}_\infty^T \\ \mathbf{V}_{2,i} & \mathbf{V}_\infty \end{bmatrix} \begin{bmatrix} \mathbf{I}_3 & \mathbf{I}_3 \\ \mathbf{Z}_{2,i} & \mathbf{Z}_\infty \end{bmatrix}^{-1}, \quad (25)$$

where

$$\mathbf{V}_{2,i} \triangleq \mathbf{Z}_{2,i} (\mathbf{A} + \mathbf{B} \mathbf{k}_2^T), \quad \mathbf{V}_\infty \triangleq \mathbf{Z}_\infty (\mathbf{A} + \mathbf{B} \mathbf{k}_\infty^T), \quad (26)$$

and

$$\begin{aligned}
\mathbf{Z}_{2,i} &\triangleq [\mathbf{0}_{3 \times 1} \quad \tilde{\mathbf{Z}}_2] [\mathbf{x}_i(0) \quad \tilde{\mathbf{E}}_{2,i}]^{-1}, \\
\mathbf{Z}_\infty &\triangleq [\mathbf{0}_{3 \times 1} \quad \tilde{\mathbf{Z}}_\infty] [\mathbf{G} \quad \tilde{\mathbf{E}}_\infty]^{-1}. \end{aligned} \quad (27)$$

$\tilde{\mathbf{E}}_{2,i}$, $\tilde{\mathbf{E}}_\infty \in \mathbb{R}^{3 \times 2}$ in (27) are such that matrices $[\mathbf{x}_i(0) \quad \tilde{\mathbf{E}}_{2,i}]$, $i \in \{2, \dots, n\}$, $[\mathbf{G} \quad \tilde{\mathbf{E}}_\infty]$, respectively, are invertible, and $\tilde{\mathbf{Z}}_2$, $\tilde{\mathbf{Z}}_\infty \in \mathbb{R}^{3 \times 2}$ are such that matrix $[\mathbf{x}_i(0) \quad \mathbf{G} \quad \tilde{\mathbf{E}}_{2,i} \quad \tilde{\mathbf{E}}_\infty] \in \mathbb{R}^{6 \times 6}$, $i \in \{2, \dots, n\}$, is invertible.

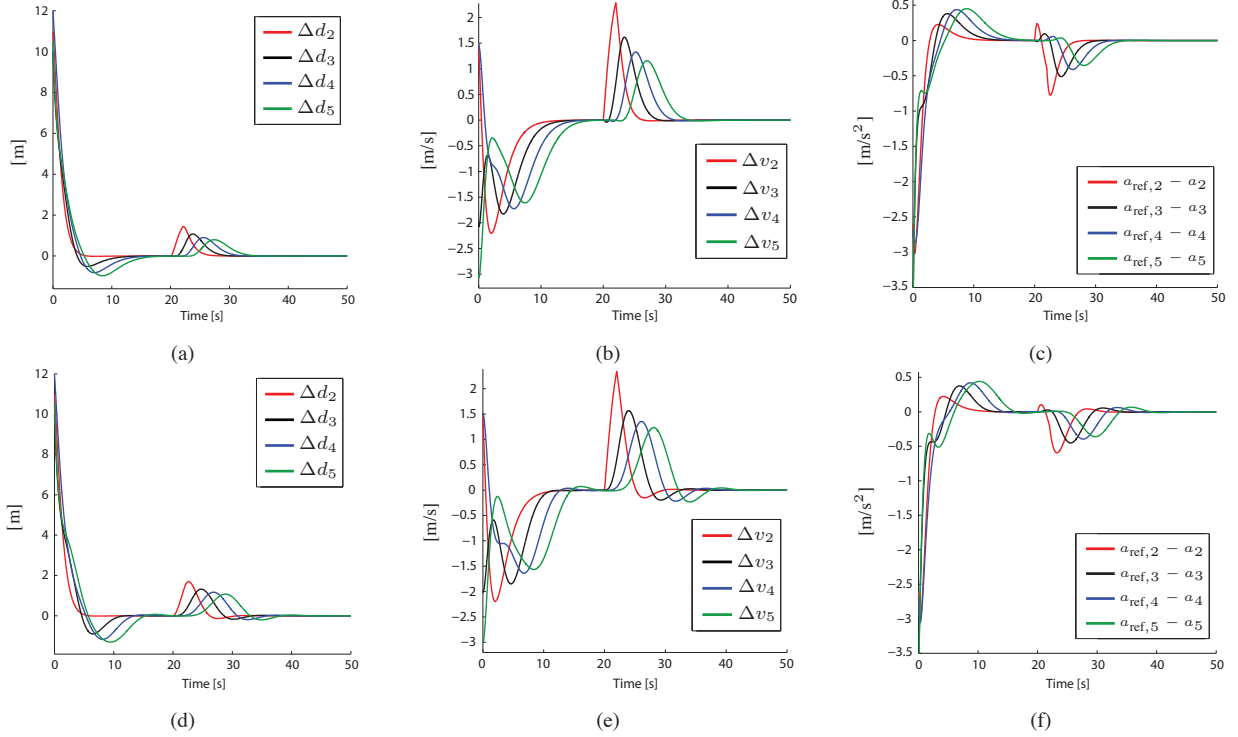


Fig. 4. *First row*, LQ regulation with guaranteed string stability; *second row*, compensator blending method. (a),(d) Time evolution of $\Delta d_i(t)$, (b),(e) of $\Delta v_i(t)$, and (c),(f) of $a_{\text{ref},i}(t) - a_i(t)$, $i \in \{2, \dots, 5\}$.

We conclude this section with Prop. 2, which provides sufficient conditions for \mathbf{k}_∞ to be stabilizing when the parameters K_L and T_L are *not exactly* known (e.g., because of an inaccurate identification of the GVLD system).

Proposition 2 (*Stabilizing \mathbf{k}_∞ with uncertain K_L, T_L*):

Let us suppose that the parameters K_L and T_L of the GVLD system (1) are not exactly known, and lie within the intervals $K_{L,m} \leq K_L \leq K_{L,M}$, $T_{L,m} \leq T_L \leq T_{L,M}$ where $K_{L,m}$, $K_{L,M}$, $T_{L,m}$ and $T_{L,M}$ are known positive constants. Then, matrix \mathbf{A} in (21) is Hurwitz if the following inequalities are satisfied:

$$\begin{aligned} K_{L,M} k_{\infty,3} < 1, \quad k_{\infty,1} \tau_h + k_{\infty,2} > 0, \quad k_{\infty,1} > 0, \\ (K_{L,m} k_{\infty,3} - 1)(k_{\infty,1} \tau_h + k_{\infty,2}) + k_{\infty,1} T_{L,M} < 0, \\ (K_{L,M} k_{\infty,3} - 1)(k_{\infty,1} \tau_h + k_{\infty,2}) + k_{\infty,1} T_{L,m} < 0. \end{aligned} \quad (28)$$

Proof: Note that the roots of the third-order polynomial (22) coincide with the roots of polynomial,

$$\frac{T_L}{K_L} \lambda^3 + \left(\frac{1}{K_L} - k_{\infty,3} \right) \lambda^2 + (k_{\infty,1} \tau_h + k_{\infty,2}) \lambda + k_{\infty,1}. \quad (29)$$

The range of variation of the coefficients of the third- and second-order term in (29), is $\frac{T_{L,m}}{K_{L,m}} \leq \frac{T_L}{K_L} \leq \frac{T_{L,M}}{K_{L,M}}$, $\frac{1}{K_{L,m}} - k_{\infty,3} \leq \frac{1}{K_L} - k_{\infty,3} \leq \frac{1}{K_{L,M}} - k_{\infty,3}$. From Kharitonov's theorem, then we have that the interval polynomial (29) is Hurwitz if and only if the following four extreme polynomials are Hurwitz,

$$p_1(\lambda) = \frac{T_{L,M}}{K_{L,m}} \lambda^3 + \left(\frac{1}{K_{L,m}} - k_{\infty,3} \right) \lambda^2 + (k_{\infty,1} \tau_h + k_{\infty,2}) \lambda + k_{\infty,1},$$

$$p_2(\lambda) = \frac{T_{L,m}}{K_{L,M}} \lambda^3 + \left(\frac{1}{K_{L,M}} - k_{\infty,3} \right) \lambda^2 + (k_{\infty,1} \tau_h + k_{\infty,2}) \lambda + k_{\infty,1},$$

$$p_3(\lambda) = \frac{T_{L,m}}{K_{L,m}} \lambda^3 + \left(\frac{1}{K_{L,m}} - k_{\infty,3} \right) \lambda^2 + (k_{\infty,1} \tau_h + k_{\infty,2}) \lambda + k_{\infty,1},$$

$$p_4(\lambda) = \frac{T_{L,M}}{K_{L,m}} \lambda^3 + \left(\frac{1}{K_{L,M}} - k_{\infty,3} \right) \lambda^2 + (k_{\infty,1} \tau_h + k_{\infty,2}) \lambda + k_{\infty,1}.$$

The application of the Routh-Hurwitz stability criterion to these polynomials, leads to (28). ■

Note that the inequalities in (28) reduce to those in (23) for $K_L = K_{L,m} = K_{L,M}$ and $T_L = T_{L,m} = T_{L,M}$, as expected.

IV. SIMULATION RESULTS

Simulation experiments have been carried out to study the performance of the control strategies described in Sect. III-A and Sect. III-B. The desired behavior of the platoon is specified in both cases by the following three performance metrics for $i \in \{2, \dots, n\}$ (cf. [7]):

- 1) *Distance and velocity tracking:* $\mathcal{C}_{T,i} = r_{\Delta d} \Delta d_i^2 + r_{\Delta v} \Delta v_i^2$ where $r_{\Delta d}$, $r_{\Delta v}$ are positive gains.
- 2) *Driver's comfort:* $\mathcal{C}_{C,i} = r_u u_i^2$ where r_u is a positive gain.
- 3) *Driver's car following:* $\mathcal{C}_{D,i} = r_a (a_{\text{ref},i} - a_i)^2$ where $a_{\text{ref},i}$ is the reference acceleration calculated according to the linear *driver's car-following model* $a_{\text{ref},i} = \kappa_D \Delta d_i + \kappa_V \Delta v_i$, and r_a , κ_D , κ_V are positive gains.

The combination of $\mathcal{C}_{T,i}$, $\mathcal{C}_{C,i}$ and $\mathcal{C}_{D,i}$ yields the following weight matrices in the quadratic cost function in (4):

$$\mathbf{Q} = \begin{bmatrix} r_{\Delta d} + \kappa_D^2 r_a & \kappa_D \kappa_V r_a & -\kappa_D r_a \\ \kappa_D \kappa_V r_a & r_{\Delta v} + \kappa_V^2 r_a & -\kappa_V r_a \\ -\kappa_D r_a & -\kappa_V r_a & r_a \end{bmatrix}, \quad r = r_u.$$

A. LQ regulation with guaranteed string stability

Figs. 4(a)-(c) shows the simulation results relative to the approach described in Sect. III-A. A platoon of 5 vehicles was simulated for 50 seconds, with $a_1(t) = 1.5 \text{ m/s}^2$ for $t \in [20, 22)$ and $a_1(t) = 0 \text{ m/s}^2$ otherwise, and with initial conditions $\mathbf{x}_2(0) = [11, 1.5, 3.2]^T$, $\mathbf{x}_3(0) = [10, -2, 3.5]^T$, $\mathbf{x}_4(0) = [12, 1.5, 3.3]^T$, $\mathbf{x}_5(0) = [10.5, -3, 3.5]^T$. The other selected parameters, are $\tau_h = 1.8\text{s}$, $T_L = 0.5\text{s}$, $K_L = 1$, $k_D = 0.02$, $k_V = 0.25$ and $r_{\Delta d} = r_{\Delta v} = 4$, $r_a = 0.1$, $r_u = 18$ (note that in CACC of cars, τ_h is typically in the subsecond time scale in the literature [11]: in our simulations,

we selected a slightly larger τ_h for improving the readability of our plots). Using (7), we obtained a feedback control gain $\mathbf{k} = [0.4714, 0.7182, -0.6038]^T$ and a feedforward control gain $k_F = -0.3110$. Figs. 4(a)-(c) show the time evolution of Δd_i , Δv_i and $a_{\text{ref},i} - a_i$, and Fig. 5 (top) the time history of u_i for $i \in \{2, \dots, 5\}$ and of a_1 . Note that with our parameters' selection, the inequalities in (11) are satisfied and the platoon is string stable. If, instead, we set $r_{\Delta d} = 1$ and keep all the other parameters unchanged, the second condition in (11) is not fulfilled anymore, thus possibly leading to a string-unstable behavior.

B. Compensator blending method

Figs. 4(d)-(f) show the simulation results relative to the approach described in Sect. III-B. In order to compare the performance of the controller designed with the compensator blending method and the LQ regulator, we repeated the simulation experiment of Sect. IV-A with the same initial conditions and parameters. We set $\mathbf{k}_2 = \mathbf{k} = [0.4714, 0.7182, -0.6038]^T$ and determined the H_∞ regulator by numerically solving in Matlab with an interior-point algorithm (the barrier method), the optimization problem $\min_{\mathbf{k}_\infty \in \mathcal{S}} \|\mathbf{k}_\infty\|_2^2$ (the initial condition is $\mathbf{k}_\infty(0) = [1, 0, 0]^T \in \mathcal{S}$), which yielded $\mathbf{k}_\infty = [0.2360, 0.2622, 0.1457]^T$. The application of the blending procedure to \mathbf{k}_2 and \mathbf{k}_∞ , led us to $\mathbf{Z}_{2,2} = \begin{bmatrix} 0.1298 & 0.6483 & -0.7502 \\ \mathbf{0}_{2 \times 3} \end{bmatrix}$, $\mathbf{Z}_{2,3} = \begin{bmatrix} -0.1855 & 0.5255 & 0.8303 \\ \mathbf{0}_{2 \times 3} \end{bmatrix}$, $\mathbf{Z}_{2,4} = \begin{bmatrix} 0.1197 & 0.6648 & -0.7373 \\ \mathbf{0}_{2 \times 3} \end{bmatrix}$, $\mathbf{Z}_{2,5} = \begin{bmatrix} -0.2616 & 0.1887 & 0.9466 \\ \mathbf{0}_{2 \times 3} \end{bmatrix}$, $\mathbf{Z}_\infty = \begin{bmatrix} 0 & 0 & 0 \\ 1 & 0 & 0 \\ 0 & 0 & 1 \end{bmatrix}$, from which the dynamic compensators \mathcal{K}_i , $i \in \{2, \dots, 5\}$, were computed using (25) and (26). Figs. 4(d)-(f) show the time evolution of Δd_i , Δv_i and $a_{\text{ref},i} - a_i$, and Fig. 5 (bottom) the time history of u_i for $i \in \{2, \dots, 5\}$ and of a_1 . From Fig. 4 we notice that the two controllers proposed in this paper achieve comparable satisfactory performances: however, from Fig. 5 (and consistently

with our choice of \mathbf{k}_∞), we can notice that the compensator blending method results in a smaller control effort.

V. CONCLUSIONS AND FUTURE WORK

In this paper we have proposed two novel *decentralized optimal* strategies for *Cooperative Adaptive Cruise Control* (CACC) of a car platoon under string-stability constraints. Some variations to the basic problem setup have also been explored and the results of numerical simulations have been provided to support our theoretical findings.

Note that the feedforward part of controller (6) does not include anticipatory characteristics for variable disturbances z_i . Any adjustment to this controller to get improved transient response usually involves lead-lag networks to replace the constant gain k_F [17]: the design of such networks will be considered in future works. In future research, we are also going to verify whether a static controller which optimally switches between \mathbf{k}_2 and \mathbf{k}_∞ may possibly outperform the dynamic regulator based on the compensator blending method, we are going to study the case of time-varying communication delays $\theta(t)$ and $\phi(t)$ [18], and to test the control strategies developed in this paper in more advanced simulation environments (e.g., in IPG's "CarMaker").

REFERENCES

- [1] D. Schrank, T. Lomax, and B. Eisele. TTI's 2011 Urban Mobility Report. Technical report, Texas Transportation Institute, The Texas A&M University System, 2011. <http://mobility.tamu.edu>.
- [2] S. Sheikholeslam and C.A. Desoer. Longitudinal Control of a Platoon of Vehicles with no Communication of Lead Vehicle Information: A System Level Study. *IEEE Trans. Contr. Syst. Tech.*, 42(4):546–554, 1993.
- [3] S.S. Stanković, M.J. Stanojević, and D.D. Šiljak. Decentralized Overlapping Control of a Platoon of Vehicles. *IEEE Trans. Contr. Syst. Tech.*, 8(5):816–832, 2000.
- [4] G. Guo and W. Yue. Autonomous Platoon Control Allowing Range-Limited Sensors. *IEEE Trans. Veh. Technol.*, 61(7):2901–2912, 2012.
- [5] G. Naus, R. van den Bleek, J. Ploeg, B. Scheepers, R. van de Molengraft, and M. Steinbuch. Explicit MPC design and performance evaluation of an ACC Stop-&-Go. In *Proc. American Contr. Conf.*, pages 224–229, 2008.
- [6] G.J. Naus, J. Ploeg, M.J. Van de Molengraft, W.P. Heemels, and M. Steinbuch. A Model Predictive Control Approach to Design a Parameterized Adaptive Cruise Control. In *Automotive Model Predictive Control: Models, Methods and Applications*, Lect. Notes Contr. Inf. Sc., chapter 17, pages 273–283. Springer, 2010.
- [7] S. Li, K. Li, R. Rajamani, and J. Wang. Model Predictive Multi-Objective Vehicular Adaptive Cruise Control. *IEEE Trans. Contr. Syst. Tech.*, 19(3):556–566, 2011.
- [8] J. Marzbanrad and N. Karimian. Space control law design in adaptive cruise control vehicles using model predictive control. *Proc. I. Mech. Eng. D-J. Aut.*, 225:870–884, 2011.
- [9] X. Liu, A. Goldsmith, S.S. Mahal, and J.K. Hedrick. Effects of communication delay on string stability in vehicle platoons. In *Proc. IEEE Int. Conf. Intell. Transp. Syst.*, pages 625–630, 2001.
- [10] D. Swaroop and K.R. Rajagopal. A review of Constant Time Headway Policy for Automatic Vehicle Following. In *Proc. IEEE Int. Conf. Intel. Trans. Syst.*, pages 65–69, 2001.
- [11] G.J.L. Naus, R.P.A. Vugts, J. Ploeg, M.J.G. van de Molengraft, and M. Steinbuch. String-Stable CACC Design and Experimental Validation: A Frequency-Domain Approach. *IEEE Trans. Veh. Technol.*, 59(9):4268–4279, 2010.
- [12] R.H. Middleton and J.H. Braslavsky. String Instability in Classes of Linear Time Invariant Formation Control with Limited Communication Range. *IEEE Trans. Automat. Contr.*, 55(7):1519–1530, 2010.
- [13] S. Öncü, N. van de Wouw, and H. Nijmeijer. Cooperative Adaptive Cruise Control: Tradeoffs Between Control and Network Specifications. In *Proc. 14th IEEE Int. Conf. Intel. Trans. Syst.*, pages 2051–2056, 2011.
- [14] F. Blanchini, P. Colaneri, and F.A. Pellegrino. Simultaneous performance achievement via compensator blending. *Automatica*, 44(1):1–14, 2008.
- [15] P. Colaneri, J.C. Geromel, and A. Locatelli. *Control theory and design: an RH_2 and RH_∞ viewpoint*. Academic Press, 1997.
- [16] J.P. Maschuw, H. Diab, D. Abel, and S. Kowalewski. Control Design for Generalized Platoon Problems. *Automatisierungstechnik*, 59(12):721–729, 2011.
- [17] B.D.O. Anderson and J.B. Moore. *Optimal Control: Linear Quadratic Methods*. Prentice-Hall International, Inc., 1989.
- [18] K. Gu, V. Kharitonov, and J. Chen. *Stability of time-delay systems*. Birkhäuser, 2003.

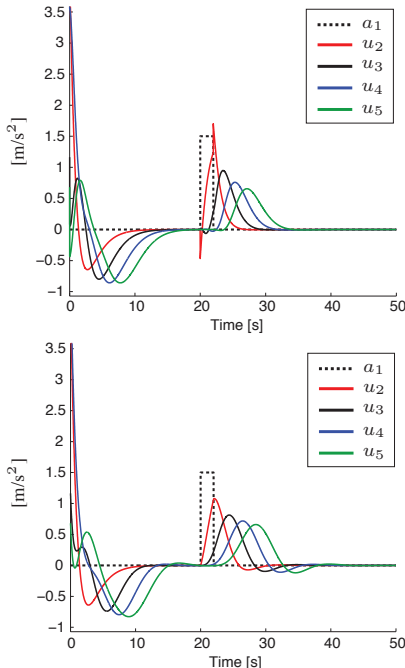


Fig. 5. Time evolution of $u_i(t)$, $i \in \{2, \dots, 5\}$, for: (top) the LQ regulator, (bottom) the regulator based on the compensator blending method.